Talanta 116 (2013) 84–90

Contents lists available at ScienceDirect

Talanta

journal homepage: www.elsevier.com/locate/talanta

Supported protein G on gold electrode: Characterization and immunosensor application

Imen Hafaiedh [a], Hanen Chammem [a], Adnane Abdelghani [a], Eric Ait [b], Laurent Feldman [c,d], Olivier Meilhac [c,e], Laurence Mora [f,*]

[a] Carthage University, Nanotechnology Laboratory, National Institute of Applied Science and Technology, Centre Urbain Nord, Bp676, 1080 Charguia Cedex, Tunisia
[b] Université Paris 13, Sorbonne Paris Cité, Laboratoire des Sciences des Procédés et des Matériaux, CNRS (UPR 3407), F-93430 Villetaneuse, France
[c] INSERM UMR698, F-75018 Paris, France
[d] Univ Paris Diderot, Sorbonne Paris Cité, F-75018 Paris, France
[e] AP-HP, Bichat Stroke Center, F-75018 Paris, France
[f] Inserm U698, Bio-ingénierie Cardiovasculaire, Institut Galilée, Université Paris 13, Sorbonne Paris Cité, F-93430 Villetaneuse, France

ARTICLE INFO

Article history:
Received 3 January 2013
Received in revised form
18 April 2013
Accepted 24 April 2013
Available online 3 May 2013

Keywords:
C-reactive protein
Antigen–antibody recognition
Cyclic voltammetry
Electrochemical impedance spectroscopy
Atomic force microscopy
Contact angle

ABSTRACT

In this work, we study the electrochemical properties of protein layer grafted on gold electrode for C-reactive protein detection. Two CRP-antibody immobilization methods were used: the first method is based on direct physisorption of CRP-antibody onto the gold surface and the second method is based on oriented CRP-antibody with protein G intermediate layer. The two developed immunosensors were tested against CRP antigen in phosphate buffer saline solution and in human plasma. The electrochemical characterization of each immobilized layers was achieved by cyclic voltammetry and impedance spectroscopy. The morphology of the deposited biomolecules was observed by Atomic Force Microscopy and the roughness was measured. Moreover, contact angle measurement was used for wettability studies. The response of the developed immunosensors was reproducible, rapid, and highly stable and a detection limit of 100 fg/mL and 10 pg/mL antigen was observed with and without protein G respectively. The developed immunosensors was used for CRP detection in human plasma.

1. Introduction

Over the last few years, sensors became increasingly developed for detection and analysis of various chemical and biological compounds in important areas such as environmental monitoring, clinical applications, security and food safety. Recently, important efforts in the field of biosensors have been directed towards the use of new nanostructured materials for biomedical applications. In this work, we intend to develop a new biosensor prototype for detection of C-reactive protein (CRP), a widely used biomarker in cardiovascular diseases. CVD remain a major cause of morbidity and mort-ality in the western world, and atherothrombotic remodeling of vascular wall is one of the main determinants of morbi-mortality, whether related to coronary artery disease [1] peripheral arterial disease or ischemic stroke. An important proportion of patients presenting acute coronary syndromes (ACS) and/or cardiac death present no prior symptoms, underlying the urgent medical need to diagnose asymptomatic patients early to prevent more severe events.

CRP is the most widely studied biomarker in atherosclerosis in general and particularly in coronary disease [2]. A small increase in CRP levels, only detectable by high sensitive tests, is associated with increased probability to undergo an acute coronary event in apparently healthy subjects, but the predictive value is small after adjustment for other classical risk factors [3]. Determination of CRP levels, albeit informative when realized shortly after an acute coronary event, is still a matter of debate as prognostic marker [4]. The Executive Summary of the Screening for Heart Attack Prevention and Education task force was called for a non-invasive screening of all asymptomatic men and women to detect and treat those with subclinical atherosclerosis [5]. This proposal highlights the importance of having biomarkers directly reflecting arterial pathophysiology instead of common risk factors (LDL, diabetes, obesity, etc.) for atherosclerosis screening.

Electrochemical impedance spectroscopy (EIS) is a powerful technique capable of detecting small changes occurring at the solution–electrode interface. Accordingly, EIS has been extensively used for the characterization of materials and surface modification procedures, as well as for the monitoring of binding events. Impedance spectroscopy combines rapid response, low detection limits, cost-effectiveness, and the possibility of performing real-

* Corresponding author. Tel.: +33 0149402035.
E-mail address: laurence.mora@univ-paris13.fr (L. Mora).

0039-9140/$ - see front matter © 2013 Elsevier B.V. All rights reserved.
http://dx.doi.org/10.1016/j.talanta.2013.04.059

time monitoring of the samples, in contrast to established strategies for pathogen detection such as cell culture, polymerase chain reaction (PCR), and enzyme linked immunosorbent assay (ELISA), or those sensors based on sandwich assay formats. In our study, the detection of CRP is based on the impedance spectroscopy technique.

Different immobilization methods for proteins have been reported in the literature [6–9] for biosensors applications, some giving rise to a random orientation of the receptor molecules immobilized on the sensor surface. In this work, we will study the electrochemical properties of protein layers grafted on gold electrode for immunosensor application. Two antibody immobilization methods were used: (1) the simple and non time-consuming physical adsorption method and (2) the oriented immobilization antibody method, which were preferred for maintaining antibody binding properties. The latter method is also simple and rapid due to the addition of only one intermediate physisorption step of G protein to orient antibodies for an optimal recognition of CRP.

2. Experimental set-up

2.1. Antibody and consumables

Bovine Serum Albumine (0.45 mg/L), Anti-CRP antibodies, purified CRP and protein G were obtained from Sigma-Aldrich (France). The buffer solution used for all experiments was phosphate buffered saline (PBS) containing 140 mM NaCl, 2.7 mM KCl, 0.1 mM Na_2HPO_4, 1.8 mM KH_2PO_4, pH=7 and the redox couple $K_4Fe(CN)_6^{3-}/K_4Fe(CN)_6^{4-}$ at a 5 mM concentration. All reagents were of analytical grade and ultrapure water (resistance 18.2 MΩ cm^{-1}) produced by a MilliporeMilli-Q system was used.

2.2. Gold cleaning and functionalization

The gold electrodes (0.16 cm^2) were produced at the LAAS of Toulouse (France). Evaporated gold (~300 nm thickness) was coated on silicon, using titanium under layer (~30 nm thickness) as a substrate. Before modification, the gold electrodes were cleaned in acetone solution for 10 min with ultrasound bath. After that, they were dried under a nitrogen flow and then dipped for 10 min into "piranha solution" 7:3 (v/v) 96% H_2SO_4/30% H_2O_2. Finally, the gold substrates were rinsed two to three times with ultrapure water and stored in ethanol solution before use.

2.3. Physisorption and oriented antibody

Random physisorption is the easiest and fastest strategy for biomolecule immobilization onto physical substrates. Among others, physisorption does not require biocomponent biotinylation, chemical modification, or the utilization of cross-linkers, and does not depend on multi-step and long experimental procedures.

For the antibody physisorption step, a 20 μg/mL Anti-CRP was deposited on the cleaned electrode and kept overnight at 4°. Finally, the electrode was treated with 1% BSA solution for 30 min to block the free spaces.

For the oriented antibody, a drop of protein G (concentration 40 μg/mL) was deposited on the cleaned gold electrode for 2 h at room temperature. The electrodes can be dried with nitrogen, then a 20 μg/mL Anti-CRP was deposited on modified electrode and left overnight at 4°. Finally, the electrode was treated with 1% BSA solution for 30 min to block the free spaces. For both cases, CRP-antigen at different concentrations was incubated on immobilized antibody for 15 min at room temperature and impedance measurement was started.

The electrodes were submitted to extensive washing with PBS after modification with the appropriate biocomponent.

2.3.1. Electrochemical set-up

2.3.1.1. Cyclic voltammetry. Cyclic voltammetry was performed at room temperature in a conventional voltammetric cell (5 mL volume) with a three electrode configuration using Voltalab40 impedance analyzer (Radiometer Analytica, France). The gold electrode (0.16 cm^2) was used as a working electrode, platinum (1 cm^2) and Ag/AgCl electrodes were used as counter and reference electrodes respectively. All the electrochemical measurements were carried out in PBS at pH 7.0 with 5 mM $K_4Fe(CN)_6^{3-}/K_4Fe(CN)_6^{4-}$ in Faraday cage [10–16] with a scan rate of 25 mV/s.

2.3.1.2. Impedance spectroscopy. In a number of reports [10–16], it has been shown that impedance spectroscopy is a useful tool to characterize the compactness of amphiphilic films on solid state surfaces. The frequency-dependent capacitance C of the complex stratified surface is related to the absolute value of the complex electric impedance Z (measured in Ohms) by the following equation:

$$|Z| = \frac{1}{2\pi f C} \quad (1)$$

where f is the frequency (in Hz) at which $|Z|$ is measured.

The surface of the device with a supported film in contact with the aqueous phase exhibits complex impedance. To fit the measured spectra with the impedance spectra out of ideal elements, we replaced the ideal elements with the constant phase elements (CPE):

$$Z_{CPE} = K\omega^{-\alpha} \quad (2)$$

The frequency exponent is $\alpha=1$ and $K=1/C$ for an ideal capacitance, and $\alpha=0$ and $K=R$ for an ideal resistance. The exponent α could be obtained, when the membrane capacitance (or layer capacitance) was replaced by a constant phase element CPE. The deviation of the exponent α from the ideal values is attributed to the inhomogeneities of the analyzed layer, like defects or roughness. The measured spectra of the impedance and phase were analyzed in terms of electrical equivalent circuits using Z_{view} software. The electric parameters of the system were calculated with the computer program and the fit error was kept under a maximum of 10%.

The impedance measurement was performed with the Voltabal40 impedance analyzer in the frequency range 0.05 Hz–100 kHz, using a modulation voltage of 10 mV. More details on electrochemical impedance spectroscopy can be found in Refs. [13–16]. The detection of the antigen was performed with impedance spectroscopy after 15 min of incubation with the final functionalized electrode.

2.3.2. Contact angle measurements

Measurements of static contact angle were made by the sessile drop method (goniometer). The measurement system was a DSA10, Krüss GmbH. Drops of 2 μL of distilled water were deposited on each sample surface using an adapted syringe. The drop images were captured and the contact angle measured using the Krüss software "Drop Shape Analysis". Before measurement, samples were rinsed in distilled water and dried under N_2. Contact angles were measured in air at room temperature.

The statistical analysis used for contact angle measurements was performed with the Student test (t-test with Excel software), $n=10$ (samples in duplicate). The probability of correlation is based on the Pearson coefficient (p), which value, when less than

0.01, corresponds to a statistically significant difference between the two populations of values that are compared.

2.3.3. Plasma samples and determination of CRP concentration by ELISA

Plasma samples were obtained from patients enrolled in the Biomarkers of Coronary Events (BIOCORE)-1 study (ClincalTrials.gov identifier: NCT00430820), a monocentric study aimed at discovering biomarkers of coronary artery disease. Blood was sampled on EDTA-containing tubes and plasma was obtained after double centrifugation (2000*g*, 10 min, 20 °C and 2500*g*, 15 min, 20 °C) as previously described [17].

2.3.4. Atomic force microscopy

AFM was used to perform topographic images of samples. The AFM machine was a nanoscope 5 (Bruker-Nano) and the cantilever was a silicon probe with aluminum reflex coating (resonant frequency: 300 kHz) and with a constant force of 40 N/m. Images were made in air, at room temperatures, and using the tapping mode. Surface morphology and roughness parameters were determined by the AFM software program. The images of topography and deflection were obtained simultaneously with a resolution of 256×256 pixels. Roughness surface was then evaluated from $10\ \mu m \times 10\ \mu m$ images.

3. Results and discussions

3.1. Biosensors based on antibody physisorption

3.1.1. Cyclic voltammetry

Cyclic voltammetry is an electrochemical technique which can be used to study the kinetic of redox reactions of materials, their insulating and conducting properties. Fig. 1 shows the cyclic voltammogram of the gold/electrolyte interface (Fig. 1a) with redox couple. Fig. 1b and c shows the cyclic voltammogram of the electrode with physisorbed antibody (Anti-CRP) and (Anti-CRP) with BSA respectively. After antibody immobilization (respectively BSA) onto the gold surface, the current decrease and the oxido-reduction peaks disappear.

3.1.2. Impedance spectroscopy

Electrochemical Impedance Spectroscopy (EIS) is an effective tool for probing the featured surface-modified electrode while controlling its electrical properties and this technique was used for example for the characterization of impedance behavior of Self Assembled Monolayers (SAMs) modified gold electrode [11–13]. Fig. 2 shows Nyquist plots for the gold electrode (Fig. 2a) after the antibody physisorption (Fig. 2b) and BSA (Fig. 2c) immobilization at 200 mV with redox couple, where Re(z) is the real part and Im (z) is the imaginary part of the complex impedance Z. The diameter of semi-circle corresponds to the charge transfer resistance of the electrode/electrolyte interface and can be fitted using the same electric model in Refs [14–17]. The CPE is the Constant Phase Element impedance of the gold/electrolyte interface, R_{ch} is the charge transfer resistance in low frequency range and W is the Warburg impedance. The resistance in high frequency ranges R_s is the resistance of the electrolyte, the contacts and connections [14–17]. All of the values of the electrical parameters are presented in Table 1. The increase of the charge transfer resistance after the antibody immobilization (respectively BSA) is due to the conductivity decreases at the gold–electrolyte interface. This confirms the results obtained with cyclic voltammetry.

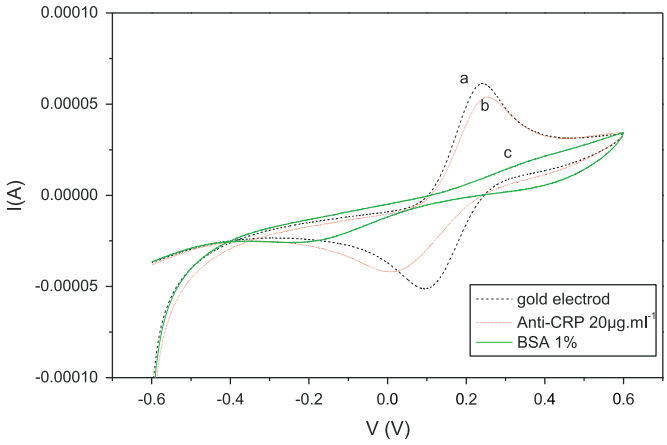

Fig. 1. Cyclic voltammograms of: (a) gold electrode; (b) gold electrode after Anti-CRP physisorption and (c) gold electrode with Anti-CRP and BSA. Scan rate of 25 mV/s, PBS solution with redox couple.

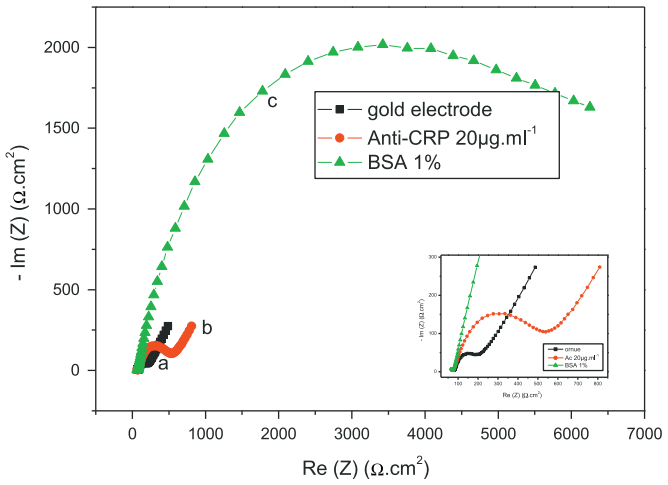

Fig. 2. Nyquist impedance plots of gold electrode after Anti-CRP physisorption and after BSA immobilization. Applied potential 200 mV, PBS solution with redox couple.

Table 1
Electric parameters obtained from fitting of the experimental results for biosensor without protein G.

Layers	R_s (Ω cm^2)	R_m (Ω cm^2)	CPE (F cm^2)	W (Ω cm^2)	α_{CPE}	X^2
Gold	78,910	130,800	9139×10^{-5}	1,740,000	0.92	0.0020
Antibody	76,510	656,500	3631×10^{-5}	1,342,000	0.91	0.0017
BSA	75,350	5506	3200×10^{-5}	2124	0.93	0.0018

3.1.3. Antigen-CRP detection

Fig. 3 shows the impedance spectra of the gold electrode functionalized with Anti-CRP (with BSA as blocking layer) before and after antigen CRP injections. The semicircle diameter in the Nyquist plot seems to decrease with the antigen concentration, implying that more amount of antigen was linked to the interface. The Anti-CRP and the CRP antigen recognition were based on Van der Waals forces of interaction. When the concentration of antigen was increased over to 100 pg/mL, the change of impedance spectra become gradually slow, showing that the immobilization of the antibody on a gold electrode tends to be saturated. A limit detection of 10 pg/mL was obtained, which was calculated according to Ref. [18].

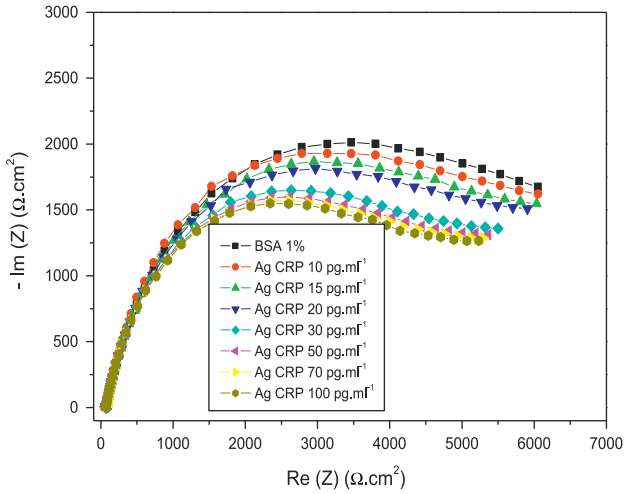

Fig. 3. Nyquist impedance plots of modified gold electrode with Anti-CRP under various concentrations of CRP antigen. Applied potential 200 mV, PBS solution with redox couple.

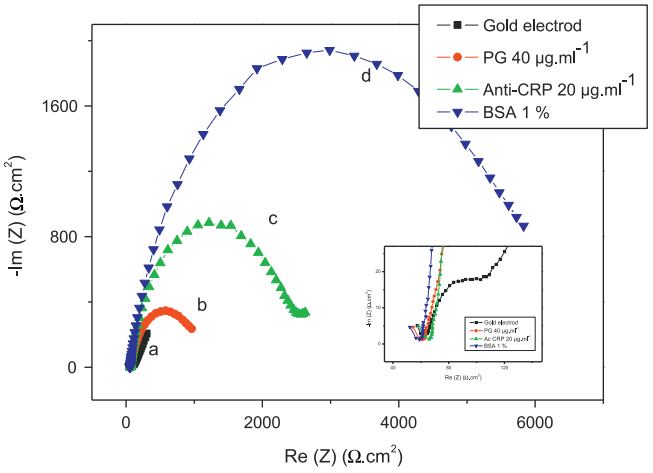

Fig. 5. Nyquist impedance plots of: (a) gold electrode; (b) gold electrode with PG; (c) gold electrode with PG and with immobilized Anti-CRP; and (d) gold electrode with PG, Anti-CRP and BSA. Applied potential 200 mV, PBS solution with redox couple.

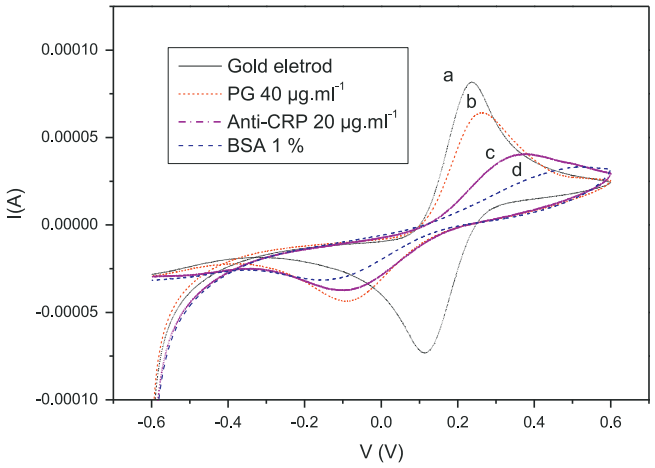

Fig. 4. Cyclic voltammograms of: (a) gold electrode; (b) gold electrode with PG; (c) gold electrode with PG and with immobilized Anti-CRP; and (d) gold electrode with PG, Anti-CRP and BSA. Scan rate of 25 mV/s, PBS solution with redox couple.

3.2. Biosensors based on oriented antibody with protein G

3.2.1. Cyclic voltammetry

Fig. 4 shows the voltammograms of the gold electrode after protein G deposition, antibody Anti-CRP and BSA immobilization in PBS buffer with 5 mM redox couple. The current decreases due to the low conductivity properties of the deposited molecules (Fig. 1b–d).

3.2.2. Impedance spectroscopy

Fig. 5 shows Nyquist plots for gold electrode after the immobilization of protein G (Fig. 5a), antibody Anti-CRP (Fig. 5b) and BSA (Fig. 5c) layers at 200 mV in PBS buffer with redox couple. The impedance spectra should be fitted using the same electric model. All of the values of the electrical parameters are presented in Table 2.

The increase of the charge transfer resistance after protein G immobilization (respectively antibody and BSA) is due to the conductivity decreases at the gold–electrolyte interface. This confirms the results obtained by cyclic voltammetry. The CPE decreases were due to the thickness increases after each step of bimolecular immobilization.

Table 2
Electric parameters obtained from fitting of the experimental results for biosensor with protein G.

Layers	R_s (Ω cm²)	R_m (Ω cm²)	CPE (F cm²)	W (Ω cm²)	α_{CPE}	X^2
Gold	58,570	88,050	6656×10^{-5}	1,589,000	0.91	0.0012
PG	62,880	899,600	5122×10^{-5}	136,900	0.90	0.0019
Antibody	66,820	2217	201×10^{-5}	950,650	0.91	0.0014
BSA	59,600	3484	1733×10^{-5}	1,581,120	0.92	0.0012

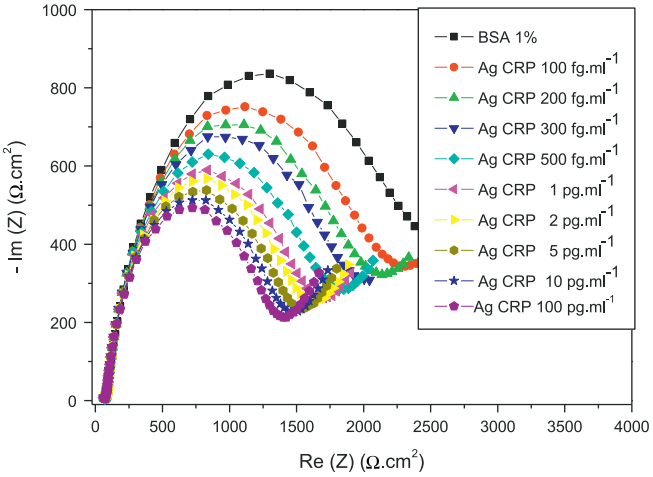

Fig. 6. Nyquist impedance plots of modified gold electrode with PG and with Anti-CRP under various concentrations of CRP-antigen. Applied potential 200 mV, PBS solution with redox couple.

3.2.3. Antigen CRP detection

Fig. 6 shows the impedance spectra of the gold electrode (modified with protein G) functionalized with Anti-CRP (with

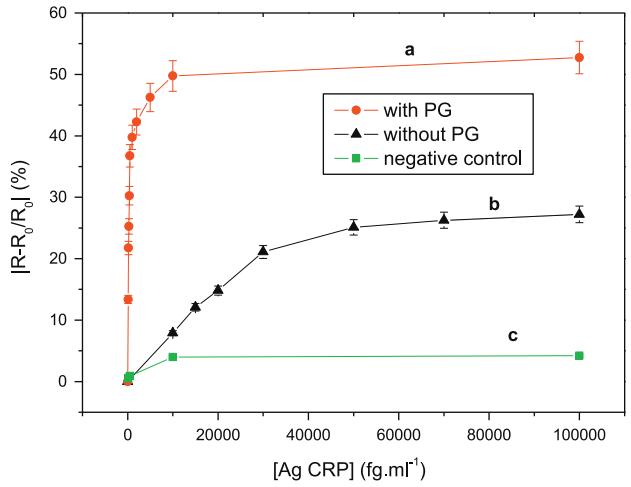

Fig. 7. Calibration curves of immunosensor with protein G (a), without protein G (b) and for specific and negative test (c).

BSA as blocking layer) before and after injection of antigen CRP concentrations. The semicircle diameter in the Nyquist plot seems to decrease with the antigen concentration, implying that more amount of antigen was linked to the interface. When the concentration of antigen was increased over 100 pg/mL, the impedance becomes gradually slow and reaches a saturated region.

The minimum CRP-antigen concentration detected was 0.1 pg/mL (100 fg/mL) with the immunosensor using protein G which contributes to specific sites orientation of the antibody. This limit detection (which was calculated according to Ref. [18]) is 100 times lower than the immunosensor without protein G. This detection limit is better than those obtained by other authors [6–8].

3.3. Calibration curves

In order to obtain the calibration data set, the values of electrode resistance variation ΔR_{ch} versus the antigen concentration of the two developed biosensors (with and without protein G) are plotted in Fig. 7a and b. The change of the charge transfer resistance is calculated following the equation:

$$DR_{ch} = |R_{ch(Ab)} - R_{ch(Ab-Ag)}|$$

where $R_{ch(Ab)}$ is the value of electrode resistance as antibody immobilized on the electrode, $R_{ch(Ab-Ag)}$ is the value of the electrode resistance after antigen binding to antibody. As shown in Fig. 7, the plot is linear and reaches a plateau for higher concentrations (saturation). A detection limit of 100 fg/mL and 10 pg/mL antigen was observed with and without protein G respectively. The reproducibility was tested against five substrates prepared in the same conditions at room temperature. The error bars which represent the standard deviation was less than 10% for the five substrates used. The stability of the immunosensor was tested against CRP antigen over 5 h. Indeed, overall measurements have been performed during 5 h and each detected concentration reached the stability in 10 min remaining stable during at least 1 h for the final measurement.

The negative control was obtained after different injection of CRP-antigen to the immunosensor coated with protein G (without the immobilized antibody, Fig. 7c). The curve shows that the charge transfer resistance remains constant due to no interaction between protein G and antigen.

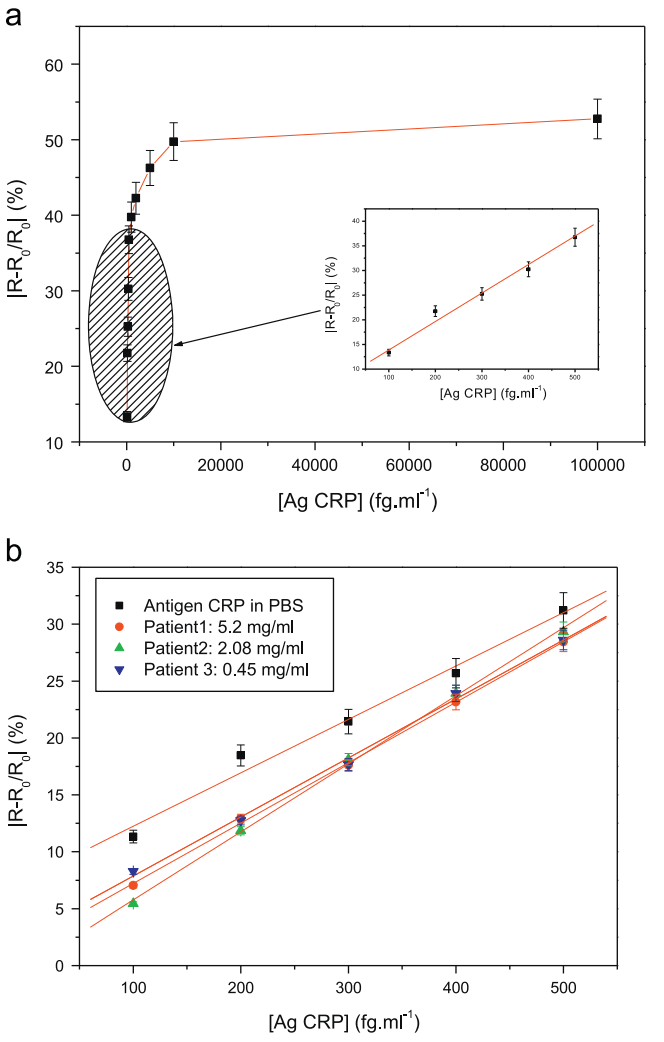

Fig. 8. Calibration curves of: (a) immunosensor with protein G for CRP-antigen detected in PBS and (b) immunosensor with protein G for CRP-antigen detected in human plasma for three patients.

3.4. Detection of CRP in human plasma from patients

Different plasma samples from three patients with coronary artery disease (Bichat Hospital, Paris, France) containing known concentrations of CRP antigen were used for impedance spectroscopy measurement (three different initial concentrations, assessed by classical particle-enhanced immunonephelometry: patient #1: 5.2 mg/L, patient #2: 2.08 mg/L and patient #3: 0.52 mg/L).

Each plasma sample was diluted to different concentrations (C_1=100 fg/mL, C_2=200 fg/mL, C_3=300 fg/mL, C_4=400 fg/mL and C_5=500 fg/mL) in order to improve detection in the linear range (at low concentration, Fig. 8a). All these concentrations from different patients were tested and compared with those detected in PBS (Fig. 8b) using the immunosensor with protein G. The obtained curves (Fig. 8b) show linear response of the immunosensor in human plasma as compared to the results obtained in PBS. The sensitivity for each calibration curves is shown in Table 3. The sensitivity of the immunosensor was nearly the same as compared to those obtained in PBS (with error bar less than 5%) with a good correlation coefficient. EIS was found to be quantitative because one should have to dilute 10 times more the sample

at 5 mg/mL than for the sample at 0.5 mg/mL to find the same EIS response in order to find the concentrations obtained by immunonephelometry.

The developed immunosensor was more sensitive than the commercially available ELISA assays (CRP) with a detection limit of 2 μg/mL in blood serum [19]. The main advantage of the impedance-based CRP immunosensor is the speed of analysis, whereas a typical ELISA needs about 4–5 h incubation time. This speed advantage is useful for quick-time measurement and analysis in emergency cases.

Table 3
Sensitivity, and correlation coefficient of immunosensor responses for CRP detected in PBS and CRP detected in plasma for each patient.

Layers	*S* (%/fg mL^{-1})	Correlation coefficient: ***R***
Ag-CRP detection in PBS	469×10^{-2}	0.99
Ag-CRP in plasma detection: 5.2 mg/L	545×10^{-2}	0.99
Ag-CRP in plasma detection: 2.08 mg/L	598×10^{-2}	0.99
Ag-CRP in plasma detection: 0.45 mg/L	518×10^{-2}	0.99

3.5. Contact angle measurements

Fig. 1 supplement summarizes contact angle values of the surfaces corresponding to each step of gold electrode functionalization. It can be seen (see ∗) that contact angles for Gold/Anti-CRP and Gold/G are not significantly different whereas they are both significantly different from Gold/G/Anti-CRP contact angle. Thus, immunoglobulins have been oriented by protein G, compared to immunoglobulins directly physisorbed on gold.

BSA (see £) has been homogeneously fixed onto Gold/G/Anti-CRP and exhibits a significantly higher value of contact angle for Gold/G/Anti-CRP/BSA (78°) compared to the previous surface Gold/G/Anti-CRP with a contact angle of 70°.

In a same way (see ∗∗), contact angle of Gold/G/Anti-CRP/BSA/antigen is significantly different than that of Gold/G/Anti-CRP/BSA. This indicates that the antigen is well fixed on Gold/G/Anti-CRP/BSA.

Finally, concerning antigen recognition by antibodies, (see §), if the antigen is loaded on gold surfaces with G/Anti-CRP/BSA or without (similar wettabillities before Ag deposition), the similar hydrophobicity (Gold and Gold/G/Anti-CRP/BSA), most significantly hydrophobic surface is that with antibodies. Thus, it can be concluded that interactions between Ag and initial surfaces are not only conditioned by hydrophobic interactions but also by

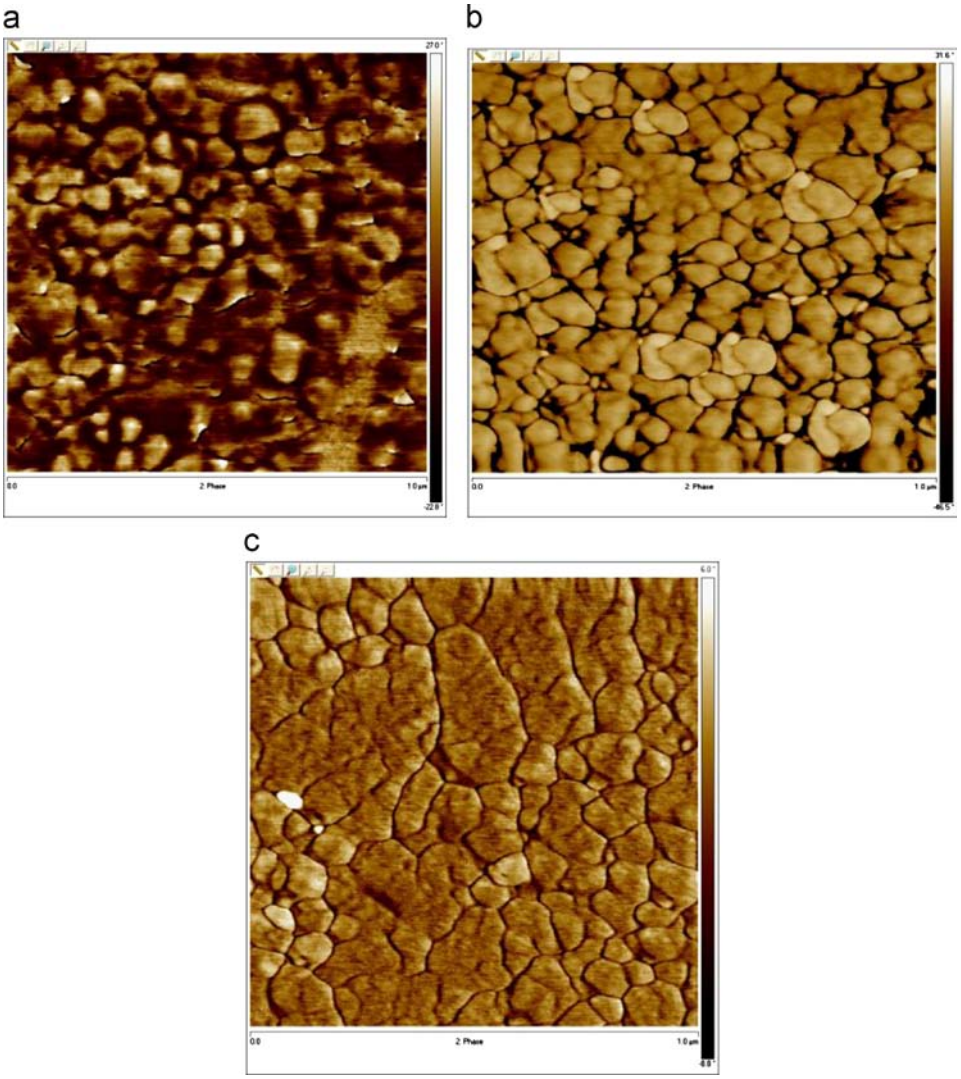

Fig. 9. AFM images in phase mode: (a) Gold, (b) Gold/G, and (c) Gold/G/Anti-CRP.

Table 4
AFM roughness of the surfaces for each step of electrode functionalization (Ra in nm) calculated with 10 × 10 images.

Gold	Gold/G	Gold/G/Anti-CRP/BSA	Gold/BSA	Gold/Anti-CRP	Gold/G/Anti-CRP/BSA/Ag	Gold/Ag	Gold/G/Anti-CRP
1.90	3.16	2.29	2.48	3.86	1.60	1.97	2.04

specific interactions in the case of Anti-CRP containing surface that orients the Ag after specific recognition.

3.6. Atomic force microscopy

Phase AFM images of substrates treated without and with protein G are shown in Fig. 2 supplement and Fig. 9. Atomic force microscopy roughness measurements were performed for each step of functionnalization (Table 4).

The Gold/Anti-CRP (Fig. 2c supplement) and Gold/G (Fig. 9b) images show the same type of morphology with coalescence of proteins with many spaces between nodules whereas no space is observed in Gold/G/Anti-CRP image (Fig. 9c). This is in agreement with wettability observations (see ∗).

Roughness measurements (Table 4) show that Anti-CRP has been oriented when loaded on G protein. Indeed, the Ra for Gold/G/Anti-CRP was found lower (2.04 nm) than for Gold/G (3.16 nm) and Gold/Anti-CRP (3.86 nm), confirming that when Anti-CRP are oriented, this leads to a lower roughness (2.04 nm) than in case of simple physisorption on Gold (3.86 nm).

Ag fixation onto the Gold/G/Anti-CRP/BSA surface is confirmed by roughness measurements: results in Table 4 show that Gold/G/Anti-CRP/BSA has an Ra of 2.29 nm and Gold/G/Anti-CRP/BSA/Ag an Ra of 1.60 nm. In a same way (see ∗∗ in Fig. 1 supplement), contact angle of Gold/G/Anti-CRP/BSA/Ag is significantly different than that of Gold/G/Anti-CRP/BSA. This indicates that Ag is well fixed on Gold/G/Anti-CRP/BSA.

4. Conclusion

In this work, we used two immobilization methods for detection of CRP by EIS-based immunosensor technology. The first method is based on oriented CRP antibodies with protein G intermediate layer. The second method is based on physisorption of CRP antibodies onto the gold surface. The electrochemical characterization of each immobilized layers was achieved with cyclic voltammetry and impedance spectroscopy. The morphology of the deposited biomolecules was evaluated by Atomic Force Microscopy and the roughness was measured. Moreover, contact angle measurement was used for analysis of wettability. A detection limit of 100 fg/mL and 10 pg/mL antigen was observed with and without protein G respectively. The developed biosensor was used for quantitative CRP detection in human plasma of healthy patients, in agreement with immunonephelometry concentrations. For future work, integrated gold microelectrodes arrays in microfluidic flow cell will be used for real time analysis.

Appendix A. Supporting information

Supplementary data associated with this article can be found in the online version at http://dx.doi.org/10.1016/j.talanta.2013.04.059.

References

[1] D.L. Bhatt, Am. J. Cardiol 98 (12A) (2006) 22Q–29Q.
[2] P.M. Ridker, Circulation 107 (2003) 363–369.
[3] J. Danesh, J.G. Wheeler, G.M. Hirschfield, S. Eda, G. Eiriksdottir, A. Rumley, G.D. Lowe, M.B. Pepys, V. Gudnason, N. Engl. J. Med. 350 (2004) 1387–1397.
[4] S. Kaptoge, E. Di Angelantonio, L Pennells, A.M. Wood, I.R. White, P. Gao, M. Walker, A. Thompson, N. Sarwar, M. Caslake, A.S. Butterworth, P. Amouyel, G. Assmann, S.J. Bakker, E.L. Barr, E. Barrett-Connor, E.J. Benjamin, C. Björkelund, H. Brenner, E Brunner, R. Clarke, J.A. Cooper, P. Cremer, M. Cushman, G.R. Dagenais, R.B. D'Agostino Sr., R. Dankner, G. Davey-Smith, D. Deeg, J.M. Dekker, G. Engström, A.R. Folsom, F.G. Fowkes, J. Gallacher, J.M. Gaziano, S. Giampaoli, R.F. Gillum, A. Hofman, B.V. Howard, E. Ingelsson, H. Iso, T. Jørgensen, S. Kiechl, A. Kitamura, Y. Kiyohara, W. Koenig, D. Kromhout, L.H. Kuller, D.A. Lawlor, T.W. Meade, A. Nissinen, B.G. Nordestgaard, A. Onat, D.B. Panagiotakos, B.M. Psaty, B. Rodriguez, A. Rosengren, V. Salomaa, J. Kauhanen, J.T. Salonen, J.A. Shaffer, S. Shea, I. Ford, C.D. Stehouwer, T.E. Strandberg, R.W. Tipping, A. Tosetto, S. Wassertheil-Smoller, P. Wennberg, R.G. Westendorp, P.H. Whincup, L. Wilhelmsen, M. Woodward, G.D. Lowe, N.J. Wareham, K.T. Khaw, N. Sattar, C.J. Packard, V. Gudnason, P.M. Ridker, M.B. Pepys, S.G. Thompson, J. Danesh, Emerging Risk Factors, N. Engl. J. Med. 367 (14) (2012) 1310–1320, http://dx.doi.org/10.1056/NEJMoa1107477. (October 4).
[5] M. Naghavi, P. Libby, E. Falk, S.W. Casscells, S. Litovsky, J. Rumberger, J.J. Badimon, C. Stefanadis, P. Moreno, G. Pasterkamp, Z. Fayad, P.H. Stone, S. Waxman, P. Raggi, M. Madjid, A. Zarrabi, A. Burke, C. Yuan, P.J. Fitzgerald, D.S. Siscovick, C.L. de Korte, M. Aikawa, K.E. Juhani Airaksinen, G. Assmann, C.R. Becker, J.H. Chesebro, A. Farb, Z.S. Galis, C. Jackson, I.K. Jang, W. Koenig, R.A. Lodder, K. March, J. Demirovic, M. Navab, S.G. Priori, M.D. Rekhter, R. Bahr, S.M. Grundy, R. Mehran, A. Colombo, E. Boerwinkle, C. Ballantyne, W. Insull, R.S. Schwartz, R. Vogel, P.W. Serruys, G.K. Hansson, D.P. Faxon, S. Kaul, H. Drexler, P. Greenland, J.E. Muller, R. Virmani, P.M. Ridker, D.P. Zipes, P.K. Shah, J.T. Willerson, Part I Circulation 108 (2003) 1664–1672.
[6] H. Hennessey, N. Afara, S. Omavonic, A.L. Padjen, Anal. Chim. Acta 643 (2009) 45–53.
[7] X. Chen, Y. Wang, J. Zhou, W. Yan, X. Li, J.-J. Zhu, Anal. Chem. 80 (2008) 2133–2140.
[8] J.J. Zhu, J.Z. Xu, J.T. He, Y.J. Wang, Q. Miao, H.Y. Chen, Anal. Lett. 36 (8) (2003) 1547–1556.
[9] G. Tanaka, H. Funabashi, M. Mie, E. Kobatake, Anal. Biochem. 350 (2) (2006) 298–303.
[10] Y. Hou, S. Helali, A. Zhang, N. Jaffrezic-Renault, C. Martelet, J. Minic, T. Gorojankina, M.-A. Persuy, E. Pajot-Augy, R. Salesse, F. Bessueille, J. Samitier, A. Errachid, V. Akimov, L. Reggiani, C. Pennetta, E. Alfinito, Biosens. Bioelectron. 21 (2006) 1393–1402.
[11] S. Hleli, A. Abdelghani, A. Tlili, Sensors 3 (2003) 472–479.
[12] S. Hleli, C. Martelet, A. Abdelghani, N. Burais, N. Jaffrezic-Renault, Sensors Actuators B 113 (2006) 711–717.
[13] J.R. MacDonald, Impedance Spectroscopy, Wiley, New York, 1987.
[14] H. Hillebrandt, A. Abdelghani, C. Abdelghani, E. Sackmann, Appl Phys A 73 (2001) 539–546.
[15] I. Hafaid, S. Chebil, H. Korri-Youssoufi, F. Bessueille, A. Errachid, Z. Sassi, Z Ali, A. Abdelghani, N. Jaffrezic-Renault, Sensors Actuators B 144 (2010) 323–331.
[16] M.B. Mejri, H. Baccar, E. Baldrich, F.J. Del Campo, S. Helali, T. Ktari, A. Simonian, M. Aouni, A. Abdelghani, Biosens. Bioelectron. 26 (4) (2010) 1261–1267.
[17] M.B. Mejri, M. Marrakchi, H. Baccar, S. Helali, M. Aouni, M. Hamdi, N. Jaffrezic-Renault, A. Abdelghani, Sensor Lett 7 (2009) 896–899.
[18] A. Shabani, M. Zourob, B. Allain, C.A Marquette, M.F Lawrence, R. Mandeville, Anal Chem 80 (24) (2008) 9475–9482.
[19] R. Dominici, P. Luraschi, C. Franzini, J. Clin. Lab. Anal. 18 (2004) (2004) 280–284.